THE JOURNAL OF BIOLOGICAL CHEMISTRY VOL. 292, NO. 3, pp. 1068–1080, January 20, 2017

A Highly Active Isoform of Lentivirus Restriction Factor SAMHD1 in Mouse*

Received for publication, June 15, 2016, and in revised form, December 1, 2016 Published, JBC Papers in Press, December 5, 2016, DOI 10.1074/jbc.M116.743740

Nicolin Bloch[‡], Sabine Gläsker[‡], Poojitha Sitaram[‡], Henning Hofmann[‡], Caitlin N. Shepard[§], Megan L. Schultz[‡], Baek Kim[§¶], and Nathaniel R. Landau[‡1]

From the [‡]Department of Microbiology, New York School of Medicine, New York, New York 10016, the [§]Center for Drug Discovery, Department of Pediatrics, Emory School of Medicine, Atlanta, Georgia 30322 , and the [¶]School of Pharmacy, Kyunghee University, Seoul 02447, South Korea

Edited by Henrik G. Dohlman

The triphosphohydrolase SAMHD1 (sterile α motif and histidine-aspartate domain-containing protein 1) restricts HIV-1 replication in nondividing myeloid cells by depleting the dNTP pool, preventing reverse transcription. SAMHD1 is also reported to have ribonuclease activity that degrades the virus genomic RNA. Human SAMHD1 is regulated by phosphorylation of its carboxyl terminus at Thr-592, which abrogates its antiviral function yet has only a small effect on its phosphohydrolase activity. In the mouse, SAMHD1 is expressed as two isoforms (ISF1 and ISF2) that differ at the carboxyl terminus due to alternative splicing of the last coding exon. In this study we characterized the biochemical and antiviral properties of the two mouse isoforms of SAMHD1. Both are antiviral in nondividing cells. Mass spectrometry analysis showed that SAMHD1 is phosphorylated at several amino acid residues, one of which (Thr-634) is homologous to Thr-592. Phosphomimetic mutation at Thr-634 of ISF1 ablates its antiviral activity yet has little effect on phosphohydrolase activity *in vitro*. dGTP caused ISF1 to tetramerize, activating its catalytic activity. In contrast, ISF2, which lacks the phosphorylation site, was significantly more active, tetramerized, and was active without added dGTP. Neither isoform nor human SAMHD1 had detectable RNase activity *in vitro* or affected HIV-1 genomic RNA stability in newly infected cells. These data support a model in which SAMHD1 catalytic activity is regulated through tetramer stabilization by the carboxyl-terminal tail, phosphorylation destabilizing the complexes and inactivating the enzyme. ISF2 may serve to reduce the dNTP pool to very low levels as a means of restricting virus replication.

The lentiviral restriction factor SAMHD1[2] is a dNTP triphosphohydrolase (1, 2) that inhibits the replication of HIV-1 in myeloid cells (3, 4). The enzyme removes the triphosphate groups of dNTPs, preventing the reverse transcription in newly infected cells (5). In addition, SAMHD1 has been proposed to have ribonuclease activity that degrades the viral genomic RNA upon virus entry (6). HIV-2 and some SIVs counteract the restriction by encoding Vpx, a virion-packaged accessory protein that induces the proteasomal degradation of SAMHD1 (3, 4, 7). Other SIVs, such as the SIV of African green monkeys, counteract SAMHD1 through the related accessory protein Vpr (8, 9). Vpx delivery into the cell by virions causes a rapid rise in the intracellular dNTP concentration, relieving the block to reverse transcription and allowing productive infection (5, 10). HIV-1 does not encode Vpx and as a result replicates poorly in dendritic and other myeloid cells. The requirement for Vpx for infection of myeloid cells can be partially replaced in culture by the addition of extracellular deoxynucleosides, which are converted into dNTPs by the salvage pathway (5). In addition, HIV-1 can be genetically modified to package Vpx, allowing it to infect myeloid cells (11, 12).

The catalytic activity of SAMHD1 is regulated by the binding of nucleotide triphosphates to two allosteric sites (allo-1 and allo-2) (1, 2, 13). The two sites differ in nucleotide binding properties such that allo-1 binds to GTP or dGTP, whereas allo-2 binds any dNTP (14–17). In the absence of bound nucleotide, SAMHD1 is dimeric. Nucleotide binding induces its tetramerization and reshapes the catalytic site to activate its phosphohydrolase activity. Mutations that prevent tetramerization by preventing allosteric binding of the activators or by disrupting the tetramer interface impair phosphohydrolase and antiviral activity (13).

SAMHD1 is also regulated by phosphorylation at residue Thr-592 by cyclin-dependent kinase 1 (CDK1), 2 (CDK2), and 6 (CDK6) (18–21). In dividing cells such as activated primary CD4+ T cells and myeloid cell-lines, SAMHD1 is hyperphosphorylated and does not restrict HIV-1 replication. In addition,

* This work was supported, in whole or in part, by National Institutes of Health Grants AI067059 and AI058864 (to N. R. L.) and AI049781 and GM104198 (to B. K.). This work was also supported by a Vilcek Fellowship Endowment Fund award (to N. B.) and an amfAR Mathilde Krim Fellowship in Basic Biomedical Research (108982-57-RKGN) and a Deutsche Forschungs Gemeinschaft post-doctoral fellowship (HO 5262/1-1; to H. H.). The authors declare that they have no conflicts of interest with the contents of this article. The content is solely the responsibility of the authors and does not necessarily represent the official views of the National Institutes of Health.

[1] To whom correspondence should be addressed: Dept. of Microbiology, NYU Langone Medical Center, Smilow Research Center, 1003, 550 First Ave, New York, NY 10016. Tel.: 212-263-9197; Fax: 212-263-9180; E-mail: nathaniel.landau@med.nyu.edu.

[2] The abbreviations used are: SAMHD1, sterile alpha motif and histidine-aspartate domain-containing protein 1; PMA, phorbol 12-myristate 13-acetate; BMDC, bone marrow-derived dendritic cell; qRT-PCR, reverse transcriptase quantitative real-time PCR; rSAMHD1, recombinant SAMHD1; rISF, recombinant ISF; SEC, size-exclusion chromatography; MALS, multi-angle light scattering; RCF, relative centrifugal force; allo-, allosteric site(s); CDK, cyclin-dependent cyclase; SIV, simian immunodeficiency virus.

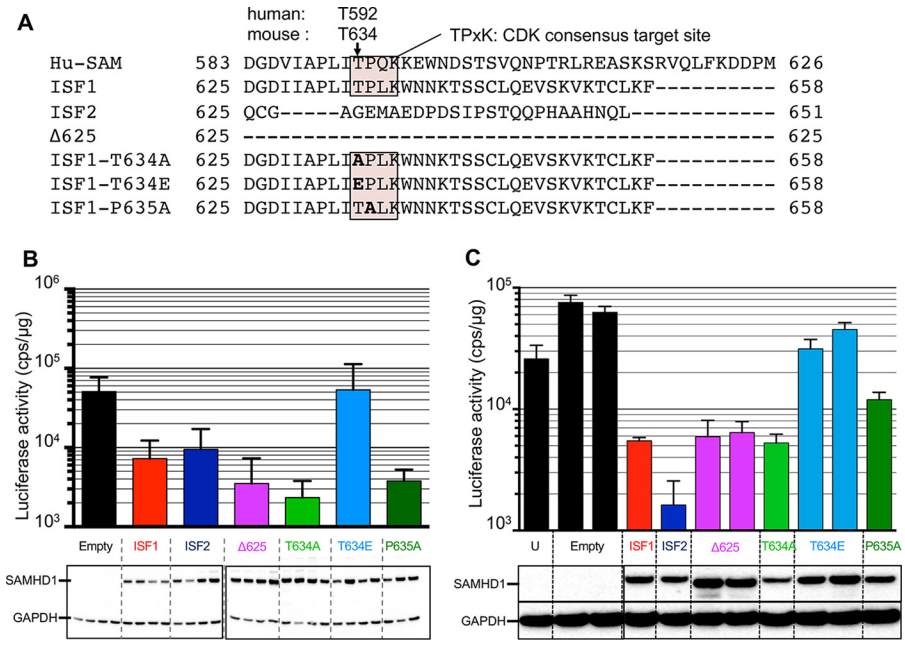

FIGURE 1. **ISF1 T634E phosphorylation site mutant lacked antiviral activity.** *A*, the amino acid sequences encoded by the last coding exon of human SAMHD1, ISF1, ISF2, and the ISF1 carboxyl-terminal mutants are shown. The phosphorylation site regulating human SAMHD1 antiviral activity, Thr-592, and its homologous residue in ISF1, Thr-634, are indicated by an *arrow*. The TP*X*K CDK2 consensus site is *boxed*. Mutated amino acids are in *bold*. *B*, U937 cells were transduced with lentiviral vectors encoding GFP, ISF1, ISF2, or mutated ISF1 (Δ625, T634A, T634E, and P635A). *B*, *top*), four single cell clones (three for P635A) were differentiated with PMA and infected with luciferase reporter HIV-1. *C*, U937 cells (*U*) were transduced with retroviral vectors encoding GFP, ISF1, ISF2, or mutated ISF1 (Δ625, T634A, T634E, and P635A). C, *top*, two single cell clones (one for ISF1, ISF2, T634A, and P635A) were differentiated with PMA and infected with luciferase reporter HIV-1. *B* and *C*, *bottom*, SAMHD1 expression was determined on the day of infection by immunoblot analysis. Representative results from two independent experiments are shown.

the phosphomimetic mutations at Thr-592 (T592D and T592E) cause SAMHD1 to lose antiviral activity. Paradoxically, the mutations prevent antiviral activity but have only a minor effect on phosphohydrolase activity *in vitro*, a finding which could argue that viral restriction requires an additional activity of SAMHD1 (19, 22). SAMHD1 has been reported to have DNase and RNase activity (23), raising the possibility that the enzyme restricts virus replication by degrading the viral genomic RNA or the newly synthesized viral DNA. The RNase activity of SAMHD1 is reported to be negatively regulated by nucleotide binding, suggesting that its antiviral activity is mediated by SAMHD1 dimers (6). The phosphohydrolase and RNase activities have been genetically separated such that mutation at D137A causes the loss of phosphohydrolase activity, whereas mutation at Q548A causes the loss of the RNase activity. Analysis of these mutated enzymes suggested that that restriction requires only the RNase activity (6, 24). These issues remain to be resolved, as the nuclease activities have been questioned in subsequent reports (25, 26).

In the mouse, SAMHD1 is expressed as two isoforms (ISF1 and ISF2) that differ in their carboxyl-terminal 30 amino acids as a result of alternative splicing of the exon 16, the last coding exon. Both isoforms are antiviral and are associated with a decrease in the intracellular dNTP pool (5). Vpx degrades neither isoform due to the altered amino acid sequence in the carboxyl-terminal Vpx binding domain. Mice are not subject to lentiviruses, and thus the role of SAMHD1 in the mouse is unclear. The myeloid cells of SAMHD1 knock-out mice are more readily infected by HIV-1 but do not appear to be more susceptible to infection by murine retroviruses (27).

To understand the function of the two SAMHD1 isoforms in the mouse, we characterized their phosphohydrolase and ribonuclease activities and their regulation by nucleotide binding, phosphorylation, and oligomerization state. We report that phosphorylation of ISF1 regulates its antiviral activity yet has only a minor effect on phosphohydrolase activity. The catalytic activity of ISF2 was much higher than ISF1 and did not require the addition of dGTP. ISF2 formed tetramers without added dGTP and was not regulated by phosphorylation. Mutations in the CDK2 phosphorylation site in the carboxyl-terminal domain of ISF1 and human SAMHD1 caused them to become dGTP-independent and tetrameric. These findings suggest a model in which SAMHD1 activity is regulated by tetramerization.

Results

Phosphorylation of ISF1 at Thr-634 Regulates Its Antiviral Activity—Human SAMHD1 is regulated by phosphorylation at amino acid Thr-592. In the mouse the homologous amino acid residue is conserved in ISF1 as Thr-634 in the CDK consensus target sequence TP*X*K. ISF2 lacks this amino acid as a result of alternative splicing of the last coding exon, which substitutes this region of the protein by an unrelated 27 amino acids (Fig. 1*A*). To understand the role of phosphorylation of the two mouse SAMHD1 isoforms, we identified the phosphorylated amino acid residues in both proteins. To do this we immunoprecipitated SAMHD1 from lysates of activated mouse splenic T cells and analyzed it by mass spectrometry. The analysis showed phosphorylation at amino acids Ser-49, Thr-52, Ser-55, Thr-56, Thr-310, and Thr-634 with frequencies ranging from 21% to 56% (Table 1), in agreement with a previous report (28).

TABLE 1
Phosphorylated amino acid residues of mouse SAMHD1
SAMHD1 was immunoprecipitated from activated mouse splenocytes, and the phosphorylated amino acid residues were identified by mass spectrometry. The ratio of phosphorylated peptides to total is shown for each amino acid.

Phosphorylated amino acids	Ratio phosphorylated peptides/total peptides	% Phosphorylated peptides
Ser-49	25/62	40
Thr-52	55/99	56
Ser-55	26/99	26
Thr-56	44/99	44
Thr-310	12/58	21
Thr-634	23/53	43

Ser-49, Thr-52, and Thr-56 are also phosphorylated in human SAMHD1 at the homologous positions (19). The role of those phosphorylations is not known, as they do not appear to regulate antiviral activity of the human enzyme (19). Phosphorylation at Ser-55 and Thr-310 appears to be unique to mouse SAMHD1, as these amino acid residues were not found in the analysis of human SAMHD1 (19). Thr-310 is not conserved in human SAMHD1 but lies in a TP*X*K CDK consensus target sequence in the mouse, indicating that it could play a significant functional role in the mouse protein. Thr-634 is homologous to Thr-592, which in human SAMHD1 is phosphorylated by CDK2 and regulates its antiviral activity, suggesting that this residue may also play an important role in the regulation of ISF1 function.

To determine the role of Thr-634 phosphorylation in regulating ISF1 antiviral activity, we generated U937 cell lines that expressed ISF1, ISF2, or carboxyl-terminal mutated ISF1. These included: Δ625 in which the sequence encoded by exon 16 was deleted; T634E, which mimics phosphorylated SAMHD1; T634A, which cannot be phosphorylated, (26, 28); P635A (Fig. 1*A*). P635A disrupts the CDK consensus phosphorylation motif and when mutated in human SAMHD1 prevents phosphorylation (19). Stable cell lines were generated by lentiviral vector transduction, and the permissiveness to HIV-1 infection of 3–4 single-cell clones with similar SAMHD1 expression levels was tested. To determine the antiviral activity of the SAMHD1 proteins, the cells were differentiated with phorbol 12-myristate 13-acetate (PMA) and then infected with luciferase reporter HIV-1 virus (Fig. 1*B*). The results showed that ISF1 and ISF2 restricted HIV-1. Δ625, T634A, and P635A retained antiviral activity, whereas T634E was inactive, consistent with previous reports (26, 28). To confirm the results, we generated single-cell clones from U937 cell lines transduced with retroviral vectors encoding each of the SAMHD1 constructs. Analysis of the cell lines showed that each construct, with the exception of T634E, restricted HIV-1 (Fig. 1*C*). To measure the dNTP triphosphohydrolase activity of the SAMHD1 forms, we immunoprecipitated the proteins from transfected 293T cells and analyzed them using an *in vitro* phosphohydrolase assay (Fig. 2*A*). We found that ISF1 was moderately active, whereas ISF2 was highly active. Introduction of the P635A mutation in ISF1 increased its catalytic activity to that of ISF2. Δ625, T634A, and T634E mutations did not alter ISF1 activity. To confirm that the lower activity of ISF1 was not simply caused by lower input of the protein in the *in vitro* assay, we repeated the assay using less ISF2. The results showed that one-fourth the amount of ISF2 retained at least as much activity as ISF1, confirming its increased catalytic activity (Fig. 2*B*).

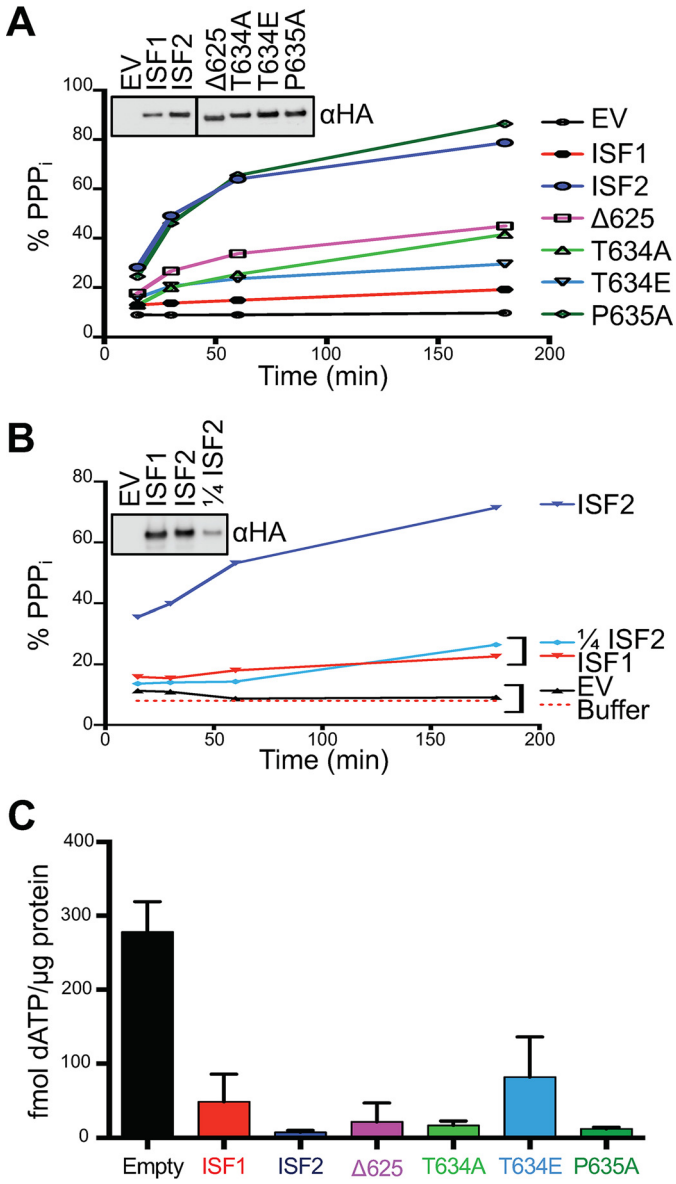

FIGURE 2. **ISF1 T634E retained catalytic activity.** *A*, 293T were transfected with empty vector (*EV*) or vector encoding ISF1, ISF2, or the mutated variants. SAMHD1 was immunoprecipitated, and its catalytic activity was measured using the *in vitro* phosphohydrolase assay. The ratio of inorganic triphosphate/(inorganic triphosphate + dATP) was plotted over time. *PPP$_i$*, inorganic triphosphate. *B*, 293T were transfected with empty vector, vectors encoding ISF1, ISF2, or ¼ of the amount of the vector encoding ISF2 (¼ ISF2). SAMHD1 was immunoprecipitated, and its catalytic activity was quantified and displayed as in *A*. *A* and *B*, *inset*, the amount of input SAMHD1 was determined by immunoblot analysis. *C*, two single-cell clones of the U937-transduced cells were differentiated with PMA, and their intracellular dATP content quantified by single nucleotide extension assay and normalized by protein content in the lysate. Representative results from one (*C*), two (*B*), and three (*A*) independent experiments are shown.

We next asked whether the reduced antiviral activity of T634E was caused by an inability of the enzyme to deplete the dNTP pool. To test this we quantified the dNTP pool in cells expressing ISF1, ISF2, or mutated forms of ISF1. We differentiated with PMA two single-cell clones of U937 cell lines expressing GFP, ISF1, ISF2, or mutated ISF1 and quantified their intracellular dATP pool (29) (Fig. 2*C*). We found that all

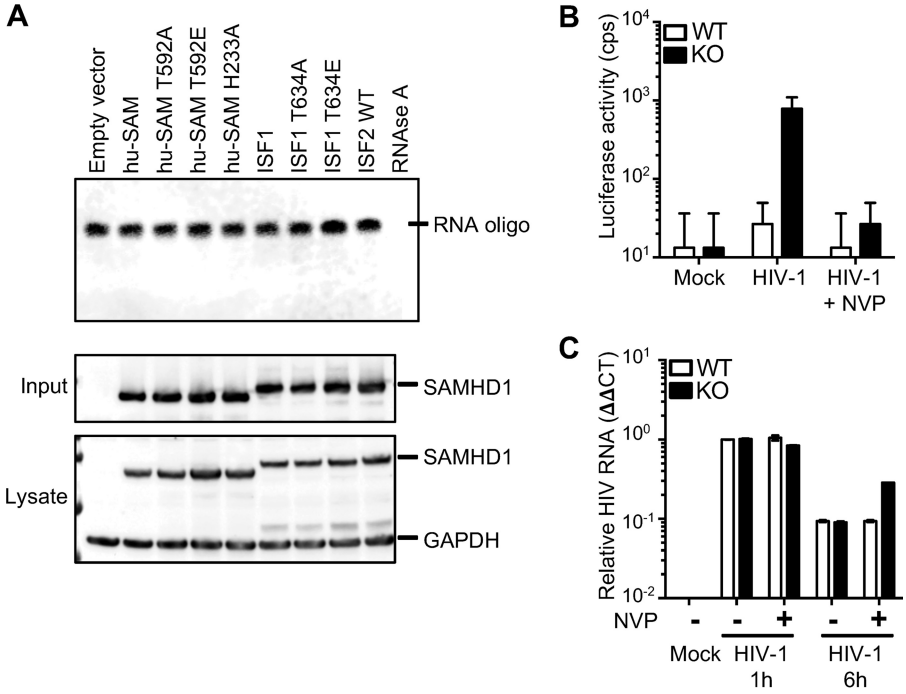

FIGURE 3. **SAMHD1 lacked detectable RNase activity.** *A*, SAMHD1 was immunoprecipitated from 293T cells transfected with empty vector (*EV*) or vectors expressing human, ISF1, ISF2, or mutated ISF1. Immunoprecipitated SAMHD1 was incubated with 5′-biotinylated oligoribonucleotide for 2 h. RNase A was added as positive control. Reactions were separated by denaturing PAGE and imaged using a streptavidin-conjugated probe. Quantification of the immunoprecipitates by immunoblot is shown in the *inset*, with GAPDH as the loading control. *B*, BMDCs from wild-type (*WT*) and SAMHD1 knock-out mice (*KO*) were infected with luciferase reporter virus in the absence or presence of nevirapine (+*NVP*). Three days post-infection, infection levels were quantified by luciferase assay. *C*, 1 and 6 h post-infection cells were collected, and RNA was prepared. The HIV-1 genomic RNA copy number was quantified by real-time qRT-PCR normalized to GAPDH mRNA, with the amount of HIV-1 RNA in wild-type cells 1 h post-infection set to one. Representative results from two independent experiments are shown.

SAMHD1 forms depleted the dNTP pool. Cells expressing ISF2 had lower dNTP levels than those expressing ISF1, in agreement with the previous finding that ISF2 has higher dNTPase activity than ISF1. Δ625, T634A, and P635A expressing cells had similar to lower dNTP levels than that of the clones encoding ISF1, in agreement with their capacity to restrict HIV-1 infection. ISF1-T634E expressing clones had slightly higher dATP levels than wild type, raising the possibility that ISF1-T634E lesser dNTP depletion failed to lower the dNTP pool to a sufficient level to block HIV-1 RT. We concluded that the carboxyl terminus of SAMHD1 regulates its catalytic activity, as its deletion lowered its activity (ISF2 compared with Δ625), whereas its modification in ISF1 increased it (ISF1 P635A compared with ISF1). As for human SAMHD1, phosphomimetic mutation at Thr-634 prevented antiviral activity without causing a major loss of phosphohydrolase activity in the *in vitro* assay.

Mouse SAMHD1 Does Not Degrade HIV-1 Genomic Viral RNA—Human SAMHD1 has been proposed to restrict HIV-1 replication by inducing the degradation of the viral genomic RNA (6, 24). To test whether this might be the case for mouse SAMHD1, we transfected 293T cells with ISF1, ISF1 T634A and T634E, ISF2, human SAMHD1 T592A and T592E, and the catalytically inactive mutant H233A (2, 13). We immunoprecipitated the proteins, incubated them with a 5′-biotinylated single-stranded RNA oligonucleotide, and analyzed the products by denaturing PAGE (Fig. 3*A*). None of the proteins caused any detectable degradation of the oligoribonucleotide, whereas a small amount of pure RNase A completely digested it.

Despite the lack of RNase activity in the *in vitro* assay, it is possible that in the cell SAMHD1 has nuclease activity or that it recruits an RNase that degrades the viral genomic RNA. To address this question, we tested whether there was a difference in the stability of HIV-1 virion RNA upon infection of wild-type and SAMHD1 knock-out mouse bone marrow-derived dendritic cells (BMDCs). We infected wild-type and SAMHD1 knock-out BMDCs with HIV-1 luciferase reporter virus in the presence and absence of the RT inhibitor nevirapine. Nevirapine served to prevent degradation of the viral RNA by HIV-1 RT RNase H and prevented the synthesis of new viral RNA transcripts. One and six h post-infection we prepared total RNA from the cells and quantified the viral RNA copy number by reverse transcriptase quantitative real-time PCR (qRT-PCR). The infectivity of the virus was confirmed in infections in the absence of nevirapine. Wild-type BMDCs were resistant to infection, whereas SAMHD1 knock-out BMDCs were infected at a 30-fold higher level, consistent with Behrendt *et al.* (27) (Fig. 3*B*). At 1 h post-infection, there was no difference between wild-type and knock-out cells in the number of viral RNA copies. At 6 h post-infection, the viral RNA copy number declined to a similar extent in the wild-type and knock-out cells (Fig. 3*C*). Nevirapine caused a slight increase in the viral RNA copy number in the knock-out cells, but the difference was not statistically different. We concluded that SAMHD1 did not affect viral RNA stability. These findings taken together with the *in vitro* assay results strongly suggested that SAMHD1-mediated restriction does not involve RNase activity.

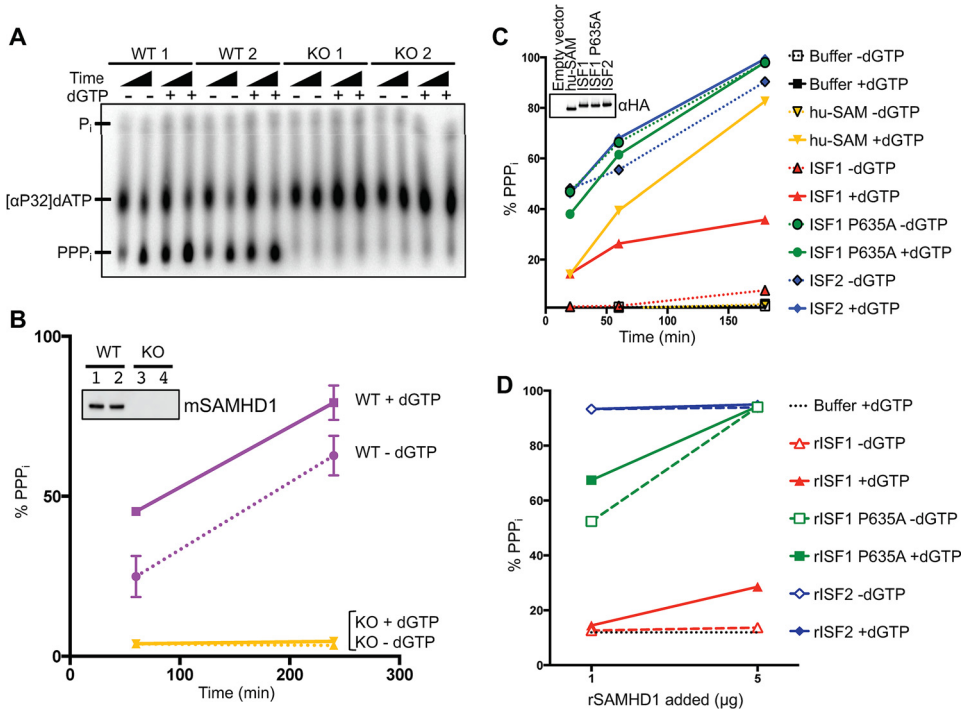

FIGURE 4. **ISF2 was dGTP-independent and highly active.** *A*, SAMHD1 was immunoprecipitated from wild-type (*WT*) or SAMHD1 knock-out (*KO*) splenocytes. Phosphohydrolase activity on [α-^{32}P]dATP was measured at 1 and 4 h in the presence or absence of dATP (−*dGTP*) or dGTP (+*dGTP*). The reaction products were separated by TLC and visualized by phosphorimaging. Inorganic triphosphate (*PPP$_i$*), inorganic monophosphate (*P$_i$*), and [α-^{32}P]dATP are indicated. *B*, the ratio of inorganic triphosphate/(inorganic triphosphate + dATP) was plotted over time. *B*, *inset*, the amount of input SAMHD1 was determined by immunoblot analysis. *C*, human SAMHD1, ISF1, ISF2, and ISF1 P635A were immunoprecipitated from transfected 293T cells, and the phosphohydrolase activity was measured. *C*, *inset*, the amount of input SAMHD1 was determined by immunoblot analysis. *D*, the phosphohydrolase activity of 1 μg and 5 μg rISF1, rISF2, and rISF1 P635A was assayed. Representative results from two (*A*, *B*, and *D*) or three (*C*) independent experiments are shown.

Mouse SAMHD1 ISF2 Has dGTP-independent Catalytic Activity—dGTP is thought to regulate the phosphohydrolase activity of human SAMHD1 as a means of activating the enzyme when dNTPs are at high concentration and shutting it off when dNTPs fall to low level. To determine whether mouse SAMHD1 is similarly regulated, we immunoprecipitated SAMHD1 from splenocytes from two wild-type and two knock-out mice. The immunoprecipitates were incubated with [α-^{32}P]dATP with or without dGTP, and after 1 and 4 h, the reaction products were analyzed by thin layer chromatography (TLC). Phosphohydrolase activity was detectable from the wild-type but not the knock-out mouse splenocytes, demonstrating the specificity of the dNTPase assay (Fig. 4, *A* and *B*). The addition of dGTP increased the phosphohydrolase activity, but unexpectedly, considerable activity was detected in the absence of dGTP.

To determine whether one or both SAMHD1 isoforms were responsible for the dGTP-independent phosphohydrolase activity, we tested the two isoforms individually. We immunoprecipitated human SAMHD1, ISF1, and ISF2 from transfected 293T cells and tested their phosphohydrolase activity (Fig. 4*C*). Human SAMHD1 lacked catalytic activity in absence of added dGTP, as previously reported (1, 2, 30). ISF1 had moderate catalytic activity that was dGTP-dependent. In contrast, ISF2 was highly active, and its activity was only slightly decreased by the absence of dGTP. We also analyzed *Escherichia coli*-produced recombinant SAMHD1 (rSAMHD1) ISF1 (rISF1) and ISF2 (rISF2) proteins. rISF1 had weak phosphohydrolase activity and was dGTP-dependent (Fig. 4*D*), whereas rISF2 had significantly higher activity that was dGTP-independent. We concluded that ISF2 is a highly active, dGTP-independent dNTPase.

ISF2 Tetramerizes in the Absence of dGTP—Human rSAMHD1 purified from *E. coli* forms dimers and is catalytically inactive (13). The addition of dGTP causes it to tetramerize, activating its catalytic activity. Our finding that ISF2 is active in the absence of dGTP could result from the formation of catalytically active dimers or from tetramerization in the absence of dGTP. To distinguish between these possibilities, we determined the oligomeric state of ISF2 in the presence and absence dGTP. For this, we incubated rISF1 and rISF2 with dGTP, dATP, or without cofactor and then covalently cross-linked the proteins. We then determined the multimeric state of the complexes by SDS-PAGE (Fig. 5*A*). In the absence of cofactor, rISF1 was mainly dimeric. The addition of dGTP induced minimal tetramerization. In contrast, rISF2 was mainly tetrameric in the presence or absence dGTP. To confirm these results, we determined the multimeric state of rISF1 and rISF2 by size-exclusion chromatography (SEC) and multi-angle light scattering (MALS). The analysis showed rISF1 formed a single low molecular mass peak of 156 kDa, whereas rISF2 was a mixture of 156- and 302 kDa forms (Fig. 5, *B* and *C*). The 156-kDa form corresponds to dimers of 77.7-kDa monomers, whereas the 302-kDa form corresponds to tetramers. Analysis of the individual SEC fractions by cross-linking showed that the higher molecular peak was mainly tetrameric, whereas the lower molecular peak was mostly dimeric (Fig. 6, *A* and *B*). Thus, ISF2, unlike ISF1, forms tetramers in the absence of dGTP.

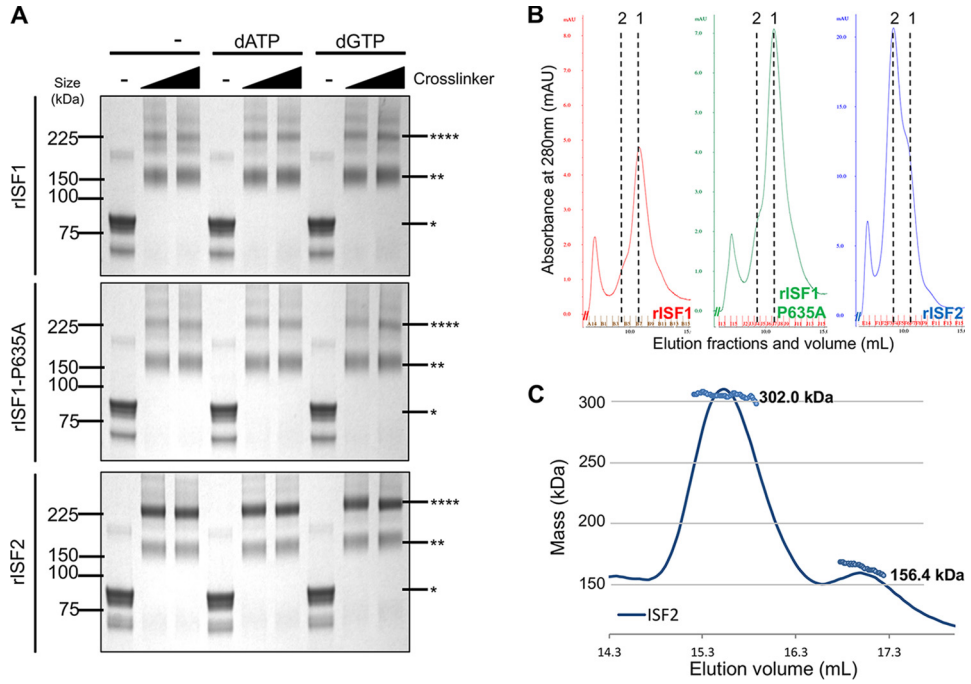

FIGURE 5. **ISF2 tetramerized in the absence of dGTP.** *A*, rISF1 (*top*), rISF1 P635A mutant (*middle*), and rISF2 (*bottom*) were cross-linked with glutaraldehyde in the absence (−) or presence of dATP or dGTP, separated by SDS-PAGE, and visualized by Coomassie staining. SAMHD1 monomers (*), dimers (**), and tetramers (****) were identified based on their molecular weight. *B*, rSAMHD1 was analyzed by SEC and detected by UV absorbance. *mAU*, milliabsorbance units. *C*, rISF2 multimers were separated by SEC, and their molecular masses were identified by inline MALS. SEC absorbance was plotted over the elution volume, and eluents for which the mass could be determined are displayed. Representative results from one (*C*) or three (*A* and *B*) independent experiments are shown.

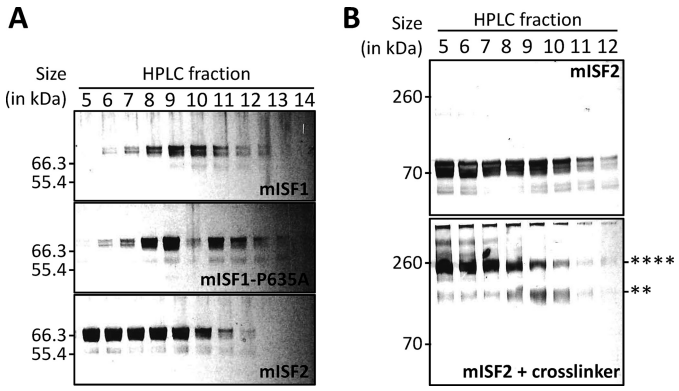

FIGURE 6. **ISF2 tetramerized in the absence of dGTP.** *A*, aliquots of each fraction eluted from the SEC from Fig. 5*B* were separated by SDS-PAGE and visualized by Coomassie staining. *B*, aliquots from each of the rISF2 SEC-eluted fractions were incubated with water (*top*) or cross-linked with glutaraldehyde (*bottom*) in the absence dGTP, then separated by SDS-PAGE and visualized by immunoblot analysis. SAMHD1 monomers, dimers (**), and tetramers (****) were identified based on their molecular weights. Representative results from two independent experiments are shown.

dGTP regulates the phosphohydrolase activity of human SAMHD1 by binding to the allosteric sites allo-1 and allo-2, inducing the dimers to tetramerize. To test whether dGTP induces ISF2 to tetramerize, we analyzed a point mutation in ISF2 allo-2 that in human SAMHD1 prevents dGTP binding (R365A) (13). To determine whether tetramerization of ISF2 is required for catalytic activity, we analyzed a double point mutation that in human SAMHD1 disrupts the tetramer interface (D393R/H396K) (13). To confirm that the allo-2 and tetramer interface mutations prevent dGTP-dependent catalytic activity of mouse SAMHD1, we introduced the mutations into ISF1 and analyzed their effect. To analyze the mutated ISF1 and ISF2, we immunoprecipitated the proteins from transfected 293T cells and measured their phosphohydrolase activity (Fig. 7). Mutation of the tetramer interface and allosteric site of ISF1 disrupted phosphohydrolase activity, confirming the effect of the mutations in the mouse protein. Mutation of the allosteric site and tetramer interface of ISF2 similarly disrupted phosphohydrolase activity. These findings suggest that, although ISF2 does not require added dGTP to be catalytically active, dGTP binding is nevertheless required for its activity.

The Carboxyl Terminus of SAMHD1 Regulates Its dGTP Dependence—The increased catalytic activity of ISF1 P635A raised the possibility that the mutation rendered the enzyme dGTP-independent. To test this possibility, we determined the effect of dGTP on the catalytic activity and multimerization state of ISF1 P635A. We found that the protein had dGTP-independent dNTPase activity (Fig. 4, *C* and *D*) yet remained dimeric in absence of dGTP (Fig. 5, *A* and *B*). This suggests that P635A ISF1 is catalytically active as a dimer. It is possible that the P635A mutation alters the conformation of the carboxyl-terminal tail in such a way that it mimics the conformational change triggered by tetramerization, activating the enzyme. To test this, we introduced the allosteric site (R365A) and interface point mutations (D393R/H396K) into ISF1 P635A and tested their catalytic activity. Both mutated proteins were catalytically inactive, demonstrating the requirement for the tetramer interface and dGTP binding. This argues for a model in which P635A changes the conformation of the carboxyl-terminal tail toward one mimicking tetramerization, activating the enzyme.

To determine whether human SAMHD1 catalytic activity is regulated in a similar fashion by its carboxyl terminus, we mutated the homologous proline residue of human SAMHD1

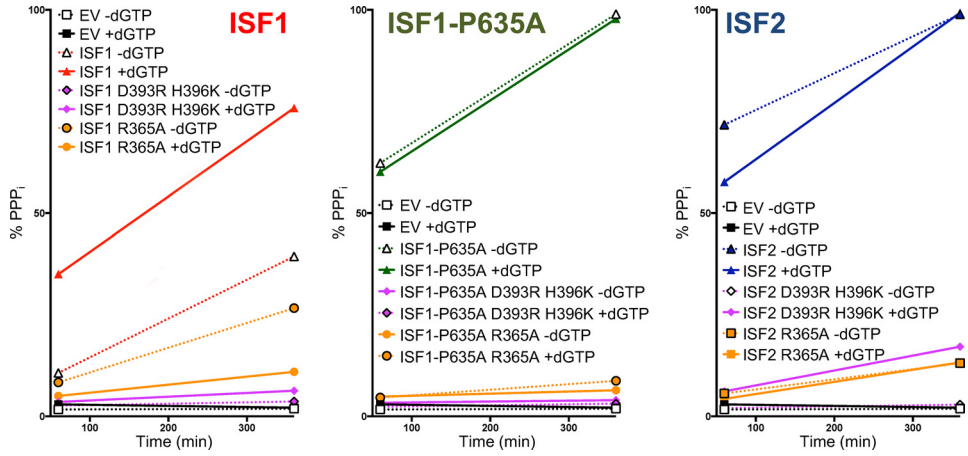

FIGURE 7. **Both of the allosteric sites and the tetramer interface were required for ISF2 phosphohydrolase activity.** ISF1, ISF1-P635A, and ISF2, wild-type SAMHD1, and mutants with disrupted allo-2 (R365A) or disrupted tetramer interface (D393R/H396K) were immunoprecipitated from transfected 293T. The phosphohydrolase activity of the immunoprecipitated SAMHD1 was quantified by phosphohydrolase assay at 1 and 6 h in presence of dATP (*−dGTP*) or dGTP (*+dGTP*). Representative results from two independent experiments are shown. *EV*, empty vector.

to alanine (P593A). Analysis of human SAMHD1 P593A showed dGTP was required to promote its tetramerization, yet its catalytic activity was dGTP-independent (Fig. 8, *A* and *B*). This suggests that the protein was active as a dimer, as was the case for ISF1 P635A (Fig. 8*C*). Mutations that disrupted the allosteric site or the tetramer interface of the protein prevented catalytic activity (data not shown), as shown for ISF1 P635A.

ISF1 and ISF2 Form dGTP-dependent Catalytically Active Heteromultimers—The presence of two isoforms that differ only at the carboxyl terminus provides the possibility that they form ISF1/ISF2 heteromultimers. To test whether the heterodimer can form, we expressed HA-tagged ISF1 with Myc-His-tagged ISF2 in 293T cells by cotransfection. We then immunoprecipitated the proteins with anti-HA or anti-Myc and determined the composition of the immunoprecipitated proteins by immunoblot analysis. We found that immunoprecipitation of either isoform led to the coimmunoprecipitation of the other, demonstrating heteromultimerization (Fig. 9*A*). To determine the catalytic properties of the ISF1/ISF2 heteromultimers, we expressed ISF1 and ISF2 together in cotransfected 293T cells and purified the heteromultimers by tandem affinity purification. For this, Myc-His-tagged ISF2 was pulled down by nickel chelate chromatography, eluted, and then pulled down with anti-HA antibody. The phosphohydrolase activity of the complexes was then measured in the presence or absence of dGTP (Fig. 9*B*). Singly expressed ISF1 was dGTP-dependent and weakly catalytic, whereas ISF2 was dGTP-independent and highly active. ISF1/ISF2 heterodimers had an intermediate level of phosphohydrolase activity that was dGTP-dependent.

Discussion

The two SAMHD1 isoforms differ by only 30 amino acids of the carboxyl-terminal domain yet have very different properties. ISF1 resembles human SAMHD1 with dGTP-dependent catalytic activity and conservation of the major negative regulatory phosphorylation site in the carboxyl-terminal domain. As for human SAMHD1, mutation of ISF1 allosteric site and of its tetramer interface disrupted its catalytic activity, demonstrating that dGTP binding and tetramerization are required for the activation of ISF1 catalytic activity. ISF2, which is specific to mouse, is more active than ISF1 or human SAMHD1 and does not require added dGTP to tetramerize and to become catalytically active. In addition, ISF2 lacks the negative regulatory phosphorylation site. Mutation of the allosteric site and of the tetramer interface of ISF2 prevented its catalytic activity. Mutations of the carboxyl terminus of ISF1 caused it to become dGTP-independent, as did the analogous mutation in human SAMHD1. These findings demonstrated the role of the carboxyl terminus in regulating SAMHD1 catalytic function.

These findings support a model in which the catalytic activity of SAMHD1 is activated by tetramerization that is regulated both by phosphorylation of the carboxyl-terminal domain and dGTP binding at the allosteric sites (Fig. 10*A*). ISF1, like the human homologue, tetramerizes upon dGTP binding, activating its catalytic activity. Phosphorylation of its carboxyl-terminal domain destabilizes the tetramer, causing it to lose activity as dGTP levels in the cell fall. ISF2 tetramerizes and is activated in the absence of added dGTP. This is likely because the enzyme as purified from *E. coli* or pulled down from mammalian cells contains dGTP that dissociates very slowly. This is likely to be the case as the catalytic activity of ISF2 requires an intact allosteric binding site; if the enzyme was truly "dGTP-independent," mutation of the dGTP binding site would have no effect on phosphohydrolase activity. This would argue that the carboxyl-terminal tail of ISF2 increases the stability of its tetramer such that when dGTP levels decline, the enzyme retains bound dGTP and remains active. ISF1/ISF2, because it has only a single carboxyl-terminal domain from ISF2, is dGTP-dependent. This model agrees with that proposed by Arnold *et al.* (31) who used ddGTP, a substrate that is hydrolyzed by SAMHD1 but does not bind the allosteric site, to show that the carboxyl-terminal domain phosphorylation does not affect SAMHD1 catalytic activity in presence of dGTP yet destabilizes the tetramer in the absence of the activator. The model predicts that ISF2, because of its high stability, can deplete the dNTP pool effectively in non-cycling cells where the rate of dNTP

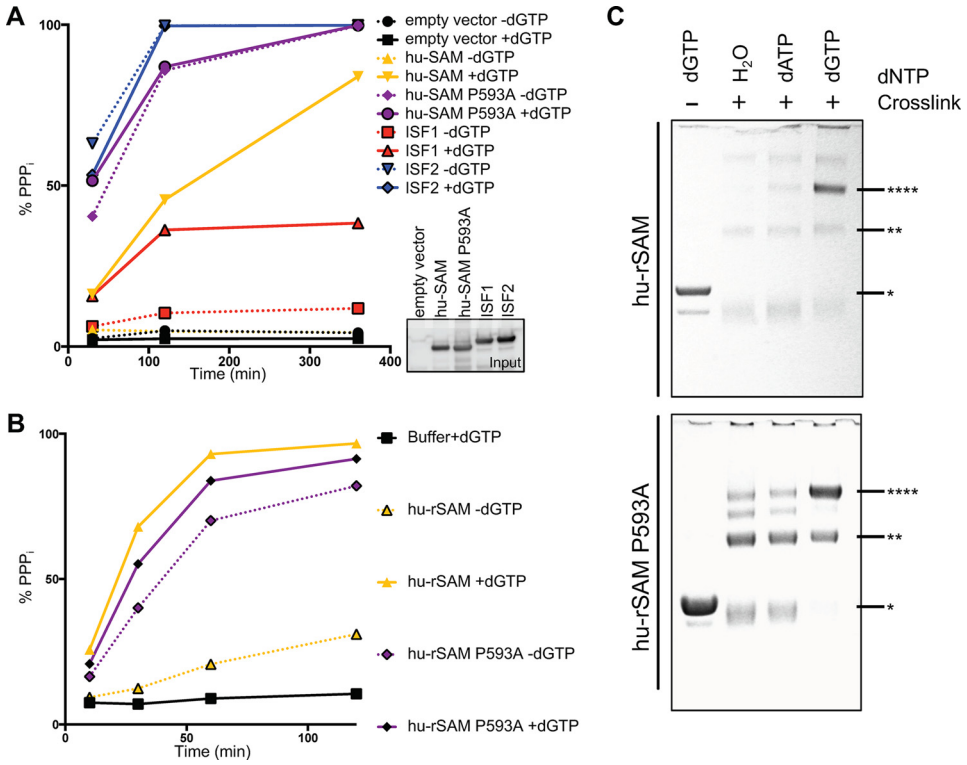

FIGURE 8. **Human SAMHD1 carboxyl terminus regulated its requirement for added dGTP to be catalytically active.** *A*, the dNTPase activity of ISF1, ISF2, human, or human P593A SAMHD1 immunoprecipitated from transfected 293T (*A*) or produced in *E. coli* (*B*) was quantified by *in vitro* phosphohydrolase assay in presence of dATP (−*dGTP*) or dGTP (+*dGTP*). The activity was plotted against the incubation duration. *A*, *inset*, SAMHD1 level in precipitates was quantified by immunoblot analysis. PPP_i, inorganic triphosphate. *C*, human rSAMHD1 (*top*) and human rSAMHD1 P593A (*bottom*) were incubated with water (−) or cross-linker (+) in the presence of water, dATP, or dGTP. Proteins were separated by SDS-PAGE and visualized by Coomassie staining. Monomers (*), dimers (**), and tetramers (****) were identified based on their respective molecular weight. Representative results from two (*B* and *C*) or three (*C*) independent experiments are shown.

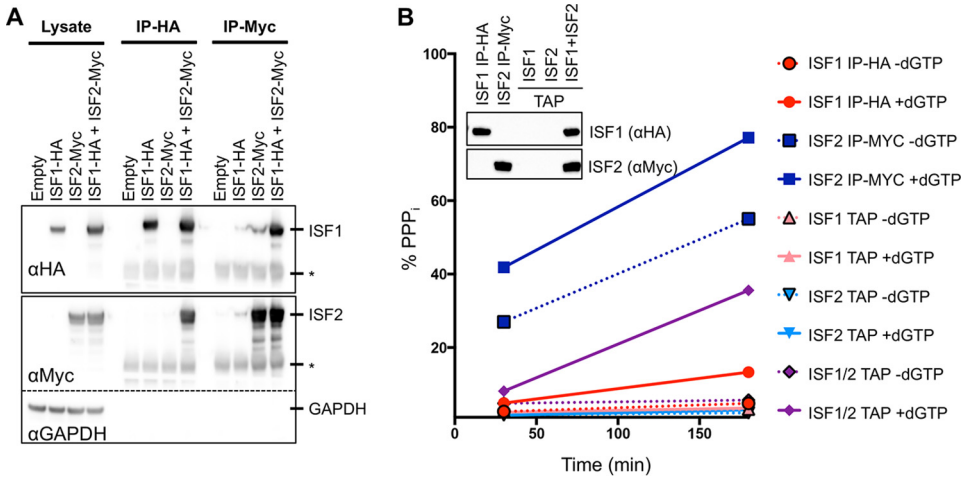

FIGURE 9. **ISF1/ISF2 multimers were dGTP-dependent and highly active.** *A*, SAMHD1 was immunoprecipitated with anti-HA (*IP-HA*)- or anti-Myc (*IP-Myc*)-coated beads from 293T transfected with HA-tagged ISF1 (*ISF1-HA*) and/or Myc-His-tagged ISF2 (*ISF2-Myc*). ISF1 and ISF2 were quantified in cell lysates and immunoprecipitates by immunoblot against HA (*ISF1*) and Myc (*ISF2*). The immunoglobulin light chain of the first antibody is visible (*). GAPDH served as the loading control for the lysates. *B*, ISF1 and ISF2 were purified as in *A*. ISF1/2 multimers were purified through a nickel pulldown of ISF2-Myc-His, then immunoprecipitation of ISF1 using anti-HA coated beads. The dNTPase activity of immunoprecipitates was quantified using the phosphohydrolase assay in the presence of dATP (−*dGTP*) or dGTP (+*dGTP*) for 45 min or 3 h. The quantified activity was plotted against the incubation duration. PPP_i, inorganic triphosphate. *B*, *inset*, ISF1 and ISF2 levels were quantified by immunoblot analysis in the immunoprecipitates. Representative results from two (*B*) or three (*A*) independent experiments are shown. PPP_i, inorganic triphosphate.

synthesis is low (Fig. 10*B*). ISF1, although less catalytically active, depletes the dNTP pool sufficiently to restrict virus replication in the cell-lines tested.

In addition to the carboxyl-terminal phosphorylation sites that we studied, mass spectrometry identified five additional phosphorylated residues in primary mouse splenocyte SAMHD1 (Ser-49, Thr-52, Ser-55, Thr-56, and Thr-310). Identical phosphorylation sites were identified by Wang *et al.* (28) at a somewhat higher frequency in transfected 293 cells expressing ISF1. The role of these sites in the regulation of SAMHD1 remains to be determined.

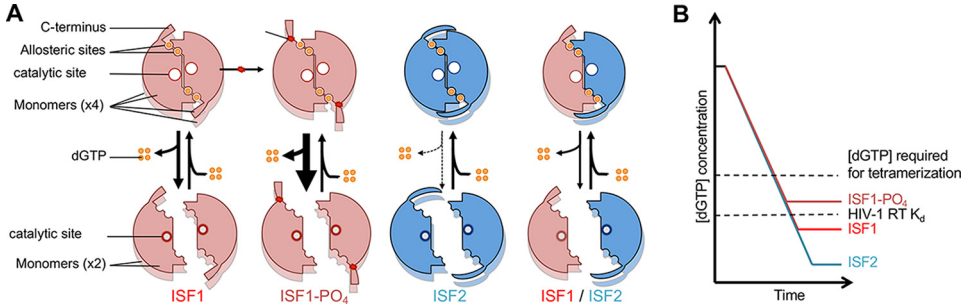

FIGURE 10. **ISF1, ISF2, and ISF1/ISF2 regulation model.** *A*, ISF1 monomers (*red*) and ISF2 (*blue*) form catalytically inactive dimers (*bottom*) due to conformational alteration in the active sites. dGTP (*orange*) binding causes tetramerization (*top*) inducing a conformational change at the active sites that activates dNTPase activity. At low dNTP concentrations dGTP is released, and the tetramers revert to inactive dimers. When the dGTP concentration is low, phosphorylation of ISF1 (ISF1-PO_4, *red*) alters the carboxyl-terminal domain conformation, destabilizing the tetramer. ISF2 has a low dGTP dissociation rate that allows the enzyme to remain tetrameric at low dNTP concentration. ISF1/ISF2 regulation is similar to that of ISF1 homodimers. *B*, the scheme of dNTP depletion accounts for the effect of ISF1 phosphorylation on antiviral activity. At low dGTP concentrations in myeloid cells, phosphorylated ISF1 (*dark red*) becomes dimeric and inactive, preventing it to deplete dNTPs below the K_D of RT. The greater stability of the unphosphorylated ISF1 (*bright red*) tetramer allows the depletion of dNTPs to a concentration that prevents reverse transcription. ISF2 tetramers are highly stable and deplete dNTPs to low levels.

The carboxyl-terminal domain of ISF1 is phosphorylated at Thr-634 by CDK1 and CDK2 (26, 28). Phosphomimetic mutation prevented antiviral activity yet had little effect on phosphohydrolase activity, a property shared by the human homologue (19, 22) and consistent with previous reports (26, 28). This finding raised the possibility that SAMHD1 does not restrict HIV-1 solely by dNTP pool depletion. Previous reports suggested that SAMHD1 has ribonuclease that degrades the viral genomic RNA in an infected cell (6, 24). Our findings do not support this possibility. We found that mammalian cell-produced SAMHD1 lacked ribonuclease activity. Furthermore, in newly infected cells SAMHD1 had no effect on the half-life of the HIV-1 genomic RNA as measured in wild-type and SAMHD1 knock-out mouse BMDCs, consistent with the findings of Wittman *et al.* (26).

A likely explanation for the effect of the carboxyl-terminal domain mutations is that they have a small effect on the phosphohydrolase activity of SAMHD1 that is difficult to detect by *in vitro* assay but that allows the dNTP concentration to rise to a level that allows reverse transcription. Consistent with this possibility, Tang *et al.* (32) and Yan *et al.* (33) reported that phosphomimetic mutants had slightly less catalytic activity than wild type, and we found that the human Thr-592 and mouse Thr-634 phosphomimetic proteins expressed in 293T cells were slightly less active than wild type, although the difference did not reach statistical significance (data not shown). Consistent with our findings, Wittman *et al.* (26) recently reported that dNTP levels were slightly higher in cells expressing the phosphomimetic mutant than in cells expressing wild-type or non-phosphorylated forms of ISF1.

SAMHD1 phosphorylation by CDK2 is thought to be a means of controlling dNTP levels through the cell cycle (33, 34), allowing the dNTP concentration to increase during S and decrease in G_1/G_0. The expression of phosphorylation site-mutated SAMHD1 caused cell cycle delay and DNA damage (33). ISF2 is similarly unregulated and thus might be expected to have negative consequences. ISF2 could cause the depletion of dNTP levels in non-cycling cells to levels below that needed to support DNA repair. However, dNTP levels are high in mouse BMDCs (35), most likely due to high RNR activity, which may protect the cells against the effect of an unregulated phosphohydrolase. Moreover, SAMHD1 did not restrict the infection and only reduced the concentration of dNTPs to a small extent in cycling cells, in agreement with a previous report (26). The formation of ISF1/ISF2 heterodimers may also play a role in mitigating the effects of ISF2. Our data suggest that mouse cells contain ISF1/ISF2 heterodimers. Because the heterodimer is dGTP-dependent, ISF2 incorporation in heterodimers may negate some of its unregulated activity. Much of the SAMHD1 activity pulled down from primary splenocytes was dGTP-independent, suggesting however, that unregulated ISF2 homodimers contribute to the activity *in vivo*.

The role of ISF2 in mouse is not clear. One possibility is that it serves to continually recycle dNTPs as a means of insuring the quality of the intracellular pool. dNTPs become oxidized as a result of ionizing radiation, and incorporation of the damaged building blocks in genomic DNA is mutagenic. The dNTP diphosphohydrolase MTH1, the catalytic activity of which is similar to SAMHD1, is thought to purge the dNTP pool of the damaged molecules (36). ISF2 could play a similar role in maintaining the quality of the dNTP pool.

Another possible role for ISF2 may be to suppress the synthesis of cytoplasmic DNA derived from endogenous retroviruses and retroelements. Knock-out of SAMHD1 in mice leads to increased expression of interferon-stimulated genes (27, 35), a phenotype that is similar to that in humans with loss-of-function mutations in *samhd1* in whom high interferon levels in cerebrospinal fluid results in an inflammatory neuropathy (37). The mechanism by which SAMHD1 knock-out results in interferon-stimulated gene induction is not known but has been proposed to be caused by the accumulation of endogenous retroelement DNA that is sensed by the cytosolic DNA sensor cyclic GMP-AMP synthase (38, 39). SAMHD1 has been found to impede the sensing of retroviral DNA by cyclic GMP-AMP synthase (40). In the mouse the ISF2 highly active isoform of SAMHD1 may be required to restrict endogenous elements because of the high burden of endogenous elements in this species. ISF2 may also play a role in protecting against other pathogenic microorganisms, including bacteria, which utilize the

intracellular dNTP pool for the synthesis of their genetic material.

Experimental Procedures

Cell Culture—293T cells were cultured in Dulbecco's modified Eagle's medium (DMEM) containing 10% fetal bovine serum (FBS) and supplemented with penicillin and streptomycin. U937 cells were cultured in RPMI 1640 supplemented with 10% FBS, penicillin, and streptomycin. BMDCs were prepared by flushing marrow cells from the femurs of C57BL/6 mice. The cells were treated with ammonium chloride/potassium chloride lysing buffer (150 mM NH_4Cl, 10 mM $KHCO_3$, 0.1 mM EDTA) and then differentiated for 6–8 days in DMEM supplemented with 10% FBS, penicillin, streptomycin, 1 mM sodium pyruvate, 2 mM L-glutamine, and 10 ng/ml granulocyte-macrophage colony-stimulating factor (Peprotech). Activated mouse T cells were prepared by treating C57BL/6 splenocytes for 3 days with 5 μg/ml concanavalin A in RPMI 1640 containing 10% FBS, 2 mM L-glutamine and 1 mM sodium pyruvate.

Mass Spectrometry—SAMHD1 was immunoprecipitated with rabbit anti-mouse SAMHD1 antibody from whole cell lysates from concanavalin A-activated splenocytes. SAMHD1 was eluted in sample buffer containing SDS, reduced with dithiothreitol, alkylated with iodoacetamide, and run onto the SDS-PAGE gel. The SAMHD1 gel band was excised and digested in-gel using trypsin. The resulting tryptic peptides were analyzed by nanoflow LC-MS using a data-dependent acquisition method on a Q Exactive mass spectrometer. The resulting MS/MS spectra were analyzed using Byonic (Protein Metrics) against the mouse SAMHD1 protein sequence. The peptides with a Byonic score <200 were excluded from further analysis. Phosphorylation of Thr-634 was manually verified.

Plasmids—Human SAMHD1 expression vector pc-hu-SAMHD1 has been previously reported (30). Murine SAMHD1 ISF1 and ISF2 expression vectors pc-mu-SAMHD1-ISF1 and pc-mu-SAMHD1-ISF2 were constructed by amplifying SAMHD1 from C57/BL6 splenocyte cDNA using a sense primer encoding a Not-I site and an HA epitope tag and an antisense primer with the carboxyl-terminal sequence of ISF1 or ISF2, including the translational termination codon followed by an Xho-I site. To construct the myc.his-tagged SAMHD1 expression vector pSAMHD1.myc.his, C57/BL6 cDNA was amplified with a 5′-primer containing a Not-I site and a 3′ primer containing an Xho-I site that generated an in-frame join to the vector-encoded myc.his tag. The amplicons were digested with Not-I and Xho-I and cloned into the Not-I and Xho-I sites of pcDNA6-A-myc.his (Invitrogen). Point mutations in the SAMHD1 expression vectors were generated by overlapping PCR, and amplicons were cloned into the Not-I and Xho-I sites of pcDNA6-A-myc.his. ISF1 and ISF2 lentiviral vectors were constructed using pLENTI-puroR (Addgene). Point mutated ISF1 and ISF2 lentiviral vectors were generated by amplifying the mutated cDNAs of the pcDNA6-A-myc.his plasmids with a sense primer containing a BamH-I site and HA epitope tag and an antisense primer containing an Xho-I site and cloning them into BamH-I and Sal-I-cleaved pLENTI-puroR. Retroviral vectors encoding ISF1, ISF1 point mutants, and ISF2 were generated by amplifying the SAMHD1 cDNAs from pLENTI-puroR-SAMHD1 with a sense primer containing a Sal-I site and an HA epitope tag and an antisense primer containing a Not-I site. The amplicons were digested with Sal-I and Not-I and cloned into the Xho-I and Not-I sites of pOZ-puroR (Addgene). Bacterial expression vectors for human, ISF1 and ISF2 strep-tagged SAMHD1, pET51.hu-SAMHD1, pET51.mu-SAMHD1.ISF1, and pET51.muSAMHD1.ISF2 were constructed by amplifying the human SAMHD1-, ISF1-, and ISF2-coding sequence from the pcDNA6 plasmids using primers containing BamH-I and Not-I sites that fused the 5′-Strep.tag sequence of pET51b+ (Novagen) to amino acid two of SAMHD1 in-frame. Amplicons were cloned into the BamH-I and Not-I sites of pET51b+. Plasmids were confirmed by nucleotide sequencing, and expression of the encoded proteins was confirmed by immunoblot analysis.

Virus and Cell Line Production—Luciferase reporter virus stocks were produced by cotransfection of 293T with pNL4.3LucE- and pVSV-G at a 5:1 ratio by the calcium phosphate method. Virus-containing supernatant was collected 48 h post transfection, filtered through a 0.45-μm pore size membrane, and concentrated 10-fold by ultracentrifugation for 90 min in a Beckman SW31 Ti rotor at 30,000 rpm through a 20% sucrose cushion, resuspended in U937 culture medium, and frozen in aliquots. The viruses were titered for luciferase activity on 293T cells, defined as cps/ml. Lentiviral vector stocks were produced by cotransfection of 293T with pLenti. SAMHD1, pMDLg/pRRE, pVSV-G, and pRSV-Rev at a ratio of 15:5:3.5:2.5. Retroviral vector stocks were produced by cotransfection of 293T with pOZ-puroR-SAMHD1, pHT-60, and pVSV-G at a ratio of 4:2:1. 48 h post-transfection virus-containing supernatants were collected, filtered, and frozen in aliquots. To establish SAMHD1-expressing U937 cell lines, 5×10^5 cells were spin-infected for 2 h at 30 °C with 1 ml of virus at 975 relative centrifugal force (RCF). The medium was changed, and 2 days later, the cells were selected in 1.0 μg/ml puromycin-supplemented medium and cloned by limiting dilution. Three or four clones (pLenti) or one to two clones (pOZ) expressing similar levels of SAMHD1 were paired for further analysis.

HIV-1 Reporter Virus Infection—SAMHD1-expressing U937 cell lines (5×10^4) were seeded in a 96-well flat-bottom plate, differentiated with 33 ng/ml PMA for 48 h, and then infected with luciferase reporter virus at 4×10^5 cps/well. Three days later luciferase activity was assayed using Steady Light Plus reagent (PerkinElmer Life Sciences), and the protein concentration was determined by Bradford assay. BMDCs from wild-type or SAMHD1 knock-out mice were plated at 1×10^5 per well in U-bottom 96-well dishes and spin-infected with 8×10^5 cps/well luciferase reporter virus for 2 h at 16 °C at 975 RCF in the presence or absence of 10 μM nevirapine. The cells were washed twice with medium and resuspended in medium with or without 10 μM nevirapine. Two days post-infection luciferase activity was measured. The data were expressed as cps normalized to the protein concentration.

Virion RNA Stability Assay—Wild-type and SAMHD1 knock-out BMDCs (3×10^6) were plated in 6-well culture dishes and spin-infected with 2.4×10^7 cps HIV-1 luciferase reporter virus per well. The cells were spin-infected at 975 × RCF for 2 h at 16 °C in the presence and absence of 10 μM

nevirapine, washed twice with cold media, then resuspended in 2 ml of medium equilibrated at 37 °C with or without 10 μM nevirapine. One and six hours later the cells were collected, and RNA was prepared using TRIzol. HIV virion genomic RNA and GAPDH mRNA transcripts were quantified by real-time qRT-PCR using SYBR Green. cDNA was synthesized with Transcriptor reverse transcriptase (Roche Applied Science) and poly(dT) primer. cDNA derived from 150 ng of RNA was amplified with primers for GAPDH (sense 5′-GGATCTGACGTGCCGCCTGG and antisense 5′-CAGCCCCGGCATCGAAGGTG) and the luciferase gene of the reporter virus (sense 5′-TGGGCGCGTTATTTATCGGA and antisense 5′-GCTGCGAAATGCCCATACTG). To control for DNA contamination, samples were included without reverse transcriptase. Copy numbers were determined using a standard curve generated by the amplification of a serial dilution of pNL-E$^-$-Luc DNA. The data were normalized to GAPDH with the number of RNA copies in the wild-type BMDCs 1 h post-infection in the absence of nevirapine set to 1.

Intracellular dNTP Pool Quantitation—dNTP pools from SAMHD1-expressing U937 cells were assessed as previously described (30). Briefly, 2×10^6 cells were differentiated with 33 ng/ml PMA for 48 h. 1/10 of the cells were lysed, and their protein content was quantified by Bradford. The remainder was lysed in 65% ice-cold methanol and dried. dNTP levels were quantified by single-nucleotide extension assay (29) and normalized to the protein content.

Preparation of rSAMHD1—E. coli BL21 (DE3) CodonPlus RIPL cells were transformed with pET51-SAMHD1 plasmids. The bacteria were induced with isopropyl-β-D-1 thiogalactopyranoside (IPTG) for 18 h at 16 °C in medium containing ampicillin and chloramphenicol. The bacteria were then pelleted by centrifugation and sonicated. Nucleic acids were removed by polyethyleneimine nucleic acid precipitation, and the rSAMHD1 protein was bound to Strep-Tactin-Sepharose (GE Healthcare) and eluted in 0.536 mg/ml D-desthiobiotin. The protein was concentrated on a Microcon 10-kDa centrifugal filter unit and analyzed by size exclusion chromatography on a Superose-12 gel filtration column. For multimerization analysis by SEC combined with inline MALS, 50 μl of rISF2 at 4.5 mg/ml was subjected to high performance liquid chromatography using a Shodex KW-803 column (JM Science, Inc.) equilibrated in SEC buffer (50 mM Tris, pH 8.0, 50 mM KCl, 5 mM $MgCl_2$). The SEC column was connected to a three-angle light-scattering detector and refractive index detector. Data were collected every second at a flow rate of 0.5 ml/min. Data were analyzed using ASTRA (Wyatt Technology) software.

In Vitro Phosphohydrolase Assay—5.0×10^6 293T cells or 3×10^8 mouse splenocytes were lysed in buffer containing 50 mM HEPES, pH 8.0, 150 mM KCl, 2 mM EDTA, 0.5% Nonidet P-40, protease inhibitor. Whole cell lysates were precleared with protein A-Sepharose (GE Healthcare) and then incubated with rabbit-anti-mouse IgG and anti-HA or anti-myc-coated protein A-Sepharose. After 2 h the beads were washed with lysis buffer followed by phosphohydrolase activity buffer (50 mM Tris, pH 8.0, 50 mM KCl, 5 mM $MgCl_2$, 0.1% Triton X-100). The beads were then incubated for the indicated times in 20 μl of phosphohydrolase activity buffer containing 0.15 μCi ([α-^{32}P]dATP and 0.4 mM dATP or 0.2 mM dATP and 0.2 mM dGTP. The reactions were heated for 5 min to 75 °C and separated by TLC on a cellulose 300 polyethyleneimine plate (Sorbent Technologies) in 1 M lithium chloride, 0.5 M formic acid. The plate was imaged on a Typhoon Trio Phosphor imager (GE Healthcare). Phosphohydrolase activity was defined as the inorganic triphosphate/(inorganic triphosphate + dATP) × 100.

For the analysis of SAMHD1 heterodimers, 293T cells were cotransfected with equal amounts of HA-ISF1 and myc.his-ISF2. After 2 days the cells were lysed in nickel-nitrilotriacetic acid lysis buffer (50 mM NaH_2PO_4/Na_2HPO_4, pH 8.0, 150 mM KCl, 0.5% Nonidet P-40, 25 mM imidazole, and protease inhibitor). The lysates were incubated for 30 min with nickel-nitrilotriacetic acid-agarose beads (Qiagen) and washed 3 times, and the bound protein was eluted in lysis buffer containing 500 mM imidazole. An equal volume of IP buffer (50 mM NaH_2PO_4/Na_2HPO_4, pH 8.0, 150 mM KCl, 0.5% Nonidet P-40) was added, and the eluted protein was immunoprecipitated with anti-HA antibody. One-fifth of the immunoprecipitate was used for immunoblot analysis, and the remainder was analyzed for phosphohydrolase activity.

In Vitro RNase Assay—HA-tagged SAMHD1 was immunoprecipitated from transfected 293T whole cell lysates. One fifth of the sample was used for immunoblot analysis, and the remainder was incubated for 15 or 120 min in 20 μl with 0.5 μM 5′-biotinylated RNA oligonucleotide (5′-CUCCAUCACCCUCCAUCACC-3′) in PBS containing 5 mM $MgCl_2$, 2 mM DTT, 10% glycerol, and 0.01% Nonidet P-40 (6). The reaction was then heated for 5 min to 75 °C, and the product was separated by 15% urea PAGE. The gel was transferred to a nylon membrane, soaked briefly in 0.1 M NaOH, and cross-linked by UV irradiation. The membrane was blocked with Tris-buffered saline/Tween 20 (TBST) containing 5% milk, probed with Dyelight 800-conjugated streptavidin, and quantified on a Licor Odyssey (LI-COR Biosciences).

Protein Cross-linking—rSAMHD1 (10 μg) or 30 μl of each eluted SEC-eluted fraction were incubated for 5 min in buffer containing 20 mM HEPES, pH 8.0, 50 mM KCl, 5 mM $MgCl_2$ with or without 0.4 mM dATP or 0.4 mM dGTP, and 7 mM glutaraldehyde (41). The reaction was quenched by adding Tris, pH 8.0, to a concentration of 250 mM. The reactions were mixed with reducing loading dye, heated for 5 min to 90 °C, and separated by Coomassie Blue-stained SDS-PAGE (pure rSAMHD1) or immunoblot analysis (SEC fractions).

Immunoblot Analysis—Immunoblots were probed with anti-GAPDH (AM4300, Life Technologies), anti Myc-tag (MMS-150P, Covance), anti-HA epitope tag (MMS-101P, Covance), or rabbit anti-mouse SAMHD1 (42) followed by horseradish peroxidase-conjugated goat anti-mouse IgG (A4416, Sigma) or goat anti-rabbit IgG antibody (A6154, Sigma) as previously described. The membranes were developed using luminescent reagents and scanned on a Licor Biosciences FC Imaging System.

Ethics Statement—The use of mouse tissues was in accordance with the recommendations of the guide for the Care and Use of Laboratory Animals of the NIH under protocols approved by the NYU School of Medicine IACUC (140303-02).

Author Contributions—N. R. L. and N. B. conceived and designed the experiments. N. B., S. G., P. S., H. H., C. N. S., and M. L. S. performed the experiments. N. B., S. G., P. S., H. H., C. N. S., B. K., and N. R. L. analyzed the data. N. B. and N. R. L. wrote the paper.

Acknowledgments—We thank Paula Jáuregui, Alice Chen, and Thomas Norton for technical assistance, Stevan R. Hubbard and Ping Cao (NYU School of Medicine) for assistance with FPLC and SEC-MALS, Shruti Nayak and Beatrix Ueberheide in the NYU School of Medicine Proteomics Resource Center for Mass Spectrometry, and Stefan Sarafianos (University of Missouri) for providing an initial batch of rSAMHD1.

References

1. Powell, R. D., Holland, P. J., Hollis, T., and Perrino, F. W. (2011) Aicardi-Goutieres syndrome gene and HIV-1 restriction factor SAMHD1 is a dGTP-regulated deoxynucleotide triphosphohydrolase. *J. Biol. Chem.* **286,** 43596–43600
2. Goldstone, D. C., Ennis-Adeniran, V., Hedden, J. J., Groom, H. C., Rice, G. I., Christodoulou, E., Walker, P. A., Kelly, G., Haire, L. F., Yap, M. W., de Carvalho, L. P., Stoye, J. P., Crow, Y. J., Taylor, I. A., and Webb, M. (2011) HIV-1 restriction factor SAMHD1 is a deoxynucleoside triphosphate triphosphohydrolase. *Nature* **480,** 379–382
3. Hrecka, K., Hao, C., Gierszewska, M., Swanson, S. K., Kesik-Brodacka, M., Srivastava, S., Florens, L., Washburn, M. P., and Skowronski, J. (2011) Vpx relieves inhibition of HIV-1 infection of macrophages mediated by the SAMHD1 protein. *Nature* **474,** 658–661
4. Laguette, N., Sobhian, B., Casartelli, N., Ringeard, M., Chable-Bessia, C., Ségéral, E., Yatim, A., Emiliani, S., Schwartz, O., and Benkirane, M. (2011) SAMHD1 is the dendritic- and myeloid-cell-specific HIV-1 restriction factor counteracted by Vpx. *Nature* **474,** 654–657
5. Lahouassa, H., Daddacha, W., Hofmann, H., Ayinde, D., Logue, E. C., Dragin, L., Bloch, N., Maudet, C., Bertrand, M., Gramberg, T., Pancino, G., Priet, S., Canard, B., Laguette, N., Benkirane, M., *et al.* (2012) SAMHD1 restricts the replication of human immunodeficiency virus type 1 by depleting the intracellular pool of deoxynucleoside triphosphates. *Nat. Immunol.* **13,** 223–228
6. Ryoo, J., Choi, J., Oh, C., Kim, S., Seo, M., Kim, S. Y., Seo, D., Kim, J., White, T. E., Brandariz-Nuñez, A., Diaz-Griffero, F., Yun, C. H., Hollenbaugh, J. A., Kim, B., Baek, D., and Ahn, K. (2014) The ribonuclease activity of SAMHD1 is required for HIV-1 restriction. *Nat. Med.* **20,** 936–941
7. Goujon, C., Jarrosson-Wuillème, L., Bernaud, J., Rigal, D., Darlix, J. L., and Cimarelli, A. (2006) With a little help from a friend: increasing HIV transduction of monocyte-derived dendritic cells with virion-like particles of SIV(MAC). *Gene Ther.* **13,** 991–994
8. Lim, E. S., Fregoso, O. I., McCoy, C. O., Matsen, F. A., Malik, H. S., and Emerman, M. (2012) The ability of primate lentiviruses to degrade the monocyte restriction factor SAMHD1 preceded the birth of the viral accessory protein Vpx. *Cell Host Microbe* **11,** 194–204
9. Laguette, N., Rahm, N., Sobhian, B., Chable-Bessia, C., Münch, J., Snoeck, J., Sauter, D., Switzer, W. M., Heneine, W., Kirchhoff, F., Delsuc, F., Telenti, A., and Benkirane, M. (2012) Evolutionary and functional analyses of the interaction between the myeloid restriction factor SAMHD1 and the lentiviral Vpx protein. *Cell Host Microbe* **11,** 205–217
10. Kim, B., Nguyen, L. A., Daddacha, W., and Hollenbaugh, J. A. (2012) Tight interplay among SAMHD1 protein level, cellular dNTP levels, and HIV-1 proviral DNA synthesis kinetics in human primary monocyte-derived macrophages. *J. Biol. Chem.* **287,** 21570–21574
11. Bobadilla, S., Sunseri, N., and Landau, N. R. (2013) Efficient transduction of myeloid cells by an HIV-1-derived lentiviral vector that packages the Vpx accessory protein. *Gene Ther.* **20,** 514–520
12. Sunseri, N., O'Brien, M., Bhardwaj, N., and Landau, N. R. (2011) Human immunodeficiency virus type 1 modified to package simian immunodeficiency virus Vpx efficiently infects macrophages and dendritic cells. *J. Virol.* **85,** 6263–6274
13. Ji, X., Wu, Y., Yan, J., Mehrens, J., Yang, H., DeLucia, M., Hao, C., Gronenborn, A. M., Skowronski, J., Ahn, J., and Xiong, Y. (2013) Mechanism of allosteric activation of SAMHD1 by dGTP. *Nat. Struct. Mol. Biol.* **20,** 1304–1309
14. Amie, S. M., Bambara, R. A., and Kim, B. (2013) GTP is the primary activator of the anti-HIV restriction factor SAMHD1. *J. Biol. Chem.* **288,** 25001–25006
15. Ji, X., Tang, C., Zhao, Q., Wang, W., and Xiong, Y. (2014) Structural basis of cellular dNTP regulation by SAMHD1. *Proc. Natl. Acad. Sci. U.S.A.* **111,** E4305–E4314
16. Koharudin, L. M., Wu, Y., DeLucia, M., Mehrens, J., Gronenborn, A. M., and Ahn, J. (2014) Structural basis of allosteric activation of sterile alpha motif and histidine-aspartate domain-containing protein 1 (SAMHD1) by nucleoside triphosphates. *J. Biol. Chem.* **289,** 32617–32627
17. Zhu, C. F., Wei, W., Peng, X., Dong, Y. H., Gong, Y., and Yu, X. F. (2015) The mechanism of substrate-controlled allosteric regulation of SAMHD1 activated by GTP. *Acta Crystallogr. D Biol. Crystallogr.* **71,** 516–524
18. Cribier, A., Descours, B., Valadão, A. L., Laguette, N., and Benkirane, M. (2013) Phosphorylation of SAMHD1 by cyclin A2/CDK1 regulates its restriction activity toward HIV-1. *Cell Rep.* **3,** 1036–1043
19. White, T. E., Brandariz-Nuñez, A., Valle-Casuso, J. C., Amie, S., Nguyen, L. A., Kim, B., Tuzova, M., and Diaz-Griffero, F. (2013) The retroviral restriction ability of SAMHD1, but not its deoxynucleotide triphosphohydrolase activity, is regulated by phosphorylation. *Cell Host Microbe* **13,** 441–451
20. Pauls, E., Ruiz, A., Badia, R., Permanyer, M., Gubern, A., Riveira-Muñoz, E., Torres-Torronteras, J., Alvarez, M., Mothe, B., Brander, C., Crespo, M., Menéndez-Arias, L., Clotet, B., Keppler, O. T., Martí, R., Posas, F., Ballana, E., and Esté, J. A. (2014) Cell cycle control and HIV-1 susceptibility are linked by CDK6-dependent CDK2 phosphorylation of SAMHD1 in myeloid and lymphoid cells. *J. Immunol.* **193,** 1988–1997
21. St Gelais, C., de Silva, S., Hach, J. C., White, T. E., Diaz-Griffero, F., Yount, J. S., and Wu, L. (2014) Identification of cellular proteins interacting with the retroviral restriction factor SAMHD1. *J. Virol.* **88,** 5834–5844
22. Welbourn, S., Dutta, S. M., Semmes, O. J., and Strebel, K. (2013) Restriction of virus infection but not catalytic dNTPase activity is regulated by phosphorylation of SAMHD1. *J. Virol.* **87,** 11516–11524
23. Beloglazova, N., Flick, R., Tchigvintsev, A., Brown, G., Popovic, A., Nocek, B., and Yakunin, A. F. (2013) Nuclease activity of the human SAMHD1 protein implicated in the Aicardi-Goutieres syndrome and HIV-1 restriction. *J. Biol. Chem.* **288,** 8101–8110
24. Choi, J., Ryoo, J., Oh, C., Hwang, S., and Ahn, K. (2015) SAMHD1 specifically restricts retroviruses through its RNase activity. *Retrovirology* **12,** 46
25. Seamon, K. J., Sun, Z., Shlyakhtenko, L. S., Lyubchenko, Y. L., and Stivers, J. T. (2015) SAMHD1 is a single-stranded nucleic acid binding protein with no active site-associated nuclease activity. *Nucleic Acids Res.* **43,** 6486–6499
26. Wittmann, S., Behrendt, R., Eissmann, K., Volkmann, B., Thomas, D., Ebert, T., Cribier, A., Benkirane, M., Hornung, V., Bouzas, N. F., and Gramberg, T. (2015) Phosphorylation of murine SAMHD1 regulates its antiretroviral activity. *Retrovirology* **12,** 103
27. Behrendt, R., Schumann, T., Gerbaulet, A., Nguyen, L. A., Schubert, N., Alexopoulou, D., Berka, U., Lienenklaus, S., Peschke, K., Gibbert, K., Wittmann, S., Lindemann, D., Weiss, S., Dahl, A., Naumann, R., *et al.* (2013) Mouse SAMHD1 has antiretroviral activity and suppresses a spontaneous cell-intrinsic antiviral response. *Cell Rep.* **4,** 689–696
28. Wang, F., St Gelais, C., de Silva, S., Zhang, H., Geng, Y., Shepard, C., Kim, B., Yount, J. S., and Wu, L. (2016) Phosphorylation of mouse SAMHD1 regulates its restriction of human immunodeficiency virus type 1 infection, but not murine leukemia virus infection. *Virology* **487,** 273–284
29. Diamond, T. L., Roshal, M., Jamburuthugoda, V. K., Reynolds, H. M., Merriam, A. R., Lee, K. Y., Balakrishnan, M., Bambara, R. A., Planelles, V., Dewhurst, S., and Kim, B. (2004) Macrophage tropism of HIV-1 depends on efficient cellular dNTP utilization by reverse transcriptase. *J. Biol. Chem.* **279,** 51545–51553
30. Hofmann, H., Logue, E. C., Bloch, N., Daddacha, W., Polsky, S. B., Schultz, M. L., Kim, B., and Landau, N. R. (2012) The Vpx lentiviral accessory

protein targets SAMHD1 for degradation in the nucleus. *J. Virol.* **86,** 12552–12560

31. Arnold, L. H., Groom, H. C., Kunzelmann, S., Schwefel, D., Caswell, S. J., Ordonez, P., Mann, M. C., Rueschenbaum, S., Goldstone, D. C., Pennell, S., Howell, S. A., Stoye, J. P., Webb, M., Taylor, I. A., and Bishop, K. N. (2015) Phospho-dependent regulation of SAMHD1 oligomerisation couples catalysis and restriction. *PLoS Pathog.* **11,** e1005194
32. Tang, C., Ji, X., Wu, L., and Xiong, Y. (2015) Impaired dNTPase activity of SAMHD1 by phosphomimetic mutation of Thr-592. *J. Biol. Chem.* **290,** 26352–26359
33. Yan, J., Hao, C., DeLucia, M., Swanson, S., Florens, L., Washburn, M. P., Ahn, J., and Skowronski, J. (2015) CyclinA2-cyclin-dependent kinase regulates SAMHD1 protein phosphohydrolase domain. *J. Biol. Chem.* **290,** 13279–13292
34. Franzolin, E., Pontarin, G., Rampazzo, C., Miazzi, C., Ferraro, P., Palumbo, E., Reichard, P., and Bianchi, V. (2013) The deoxynucleotide triphosphohydrolase SAMHD1 is a major regulator of DNA precursor pools in mammalian cells. *Proc. Natl. Acad. Sci. U.S.A.* **110,** 14272–14277
35. Rehwinkel, J., Maelfait, J., Bridgeman, A., Rigby, R., Hayward, B., Liberatore, R. A., Bieniasz, P. D., Towers, G. J., Moita, L. F., Crow, Y. J., Bonthron, D. T., and Reis e and Sousa, C. (2013) SAMHD1-dependent retroviral control and escape in mice. *EMBO J.* **32,** 2454–2462
36. Yoshimura, D., Sakumi, K., Ohno, M., Sakai, Y., Furuichi, M., Iwai, S., and Nakabeppu, Y. (2003) An oxidized purine nucleoside triphosphatase, MTH1, suppresses cell death caused by oxidative stress. *J. Biol. Chem.* **278,** 37965–37973
37. Rice, G. I., Bond, J., Asipu, A., Brunette, R. L., Manfield, I. W., Carr, I. M., Fuller, J. C., Jackson, R. M., Lamb, T., Briggs, T. A., Ali, M., Gornall, H., Couthard, L. R., Aeby, A., Attard-Montalto, S. P., *et al.* (2009) Mutations involved in Aicardi-Goutieres syndrome implicate SAMHD1 as regulator of the innate immune response. *Nat. Genet.* **41,** 829–832
38. Gao, D., Wu, J., Wu, Y. T., Du, F., Aroh, C., Yan, N., Sun, L., and Chen, Z. J. (2013) Cyclic GMP-AMP synthase is an innate immune sensor of HIV and other retroviruses. *Science* **341,** 903–906
39. Sun, L., Wu, J., Du, F., Chen, X., and Chen, Z. J. (2013) Cyclic GMP-AMP synthase is a cytosolic DNA sensor that activates the type I interferon pathway. *Science* **339,** 786–791
40. Maelfait, J., Bridgeman, A., Benlahrech, A., Cursi, C., and Rehwinkel, J. (2016) Restriction by SAMHD1 limits cGAS/STING-dependent innate and adaptive immune responses to HIV-1. *Cell Rep.* **16,** 1492–1501
41. Yan, J., Kaur, S., DeLucia, M., Hao, C., Mehrens, J., Wang, C., Golczak, M., Palczewski, K., Gronenborn, A. M., Ahn, J., and Skowronski, J. (2013) Tetramerization of SAMHD1 is required for biological activity and inhibition of HIV infection. *J. Biol. Chem.* **288,** 10406–10417
42. Zhang, R., Bloch, N., Nguyen, L. A., Kim, B., and Landau, N. R. (2014) SAMHD1 restricts HIV-1 replication and regulates interferon production in mouse myeloid cells. *PLoS ONE* **9,** e89558